PERGAMON

Computers and Structures 79 (2001) 2847–2861

Computers & Structures

www.elsevier.com/locate/compstruc

Seismically isolated bridge piers on shallow soil stratum with soil–structure interaction

A.G. Vlassis [a,*], C.C. Spyrakos [b,*]

[a] Department of Civil Engineering, University of Nevada-Reno, Reno, NV 89557, USA

[b] Earthquake Engineering Laboratory, Department of Civil Engineering, Polytechnic Campus, National Technical University of Athens, Zografos, 15700 Athens, Greece

Received 2 October 2000; accepted 27 June 2001

Abstract

The objective of this study is to assess the effects of soil–structure interaction on the response of seismically isolated bridge piers founded on a shallow soil stratum overlying a rigid bedrock and to develop a method that considers soil–structure interaction and can be easily applied to the preliminary design of bridges. The relative importance of several parameters of the bridge-isolators-soil system is examined. Cases in which soil–structure interaction needs to be incorporated in seismically isolated bridge design are identified and ways to take advantage of soil–structure interaction in order to enhance the safety level and reduce design costs are recommended. © 2001 Published by Elsevier Science Ltd.

Keywords: Bridge pier; Soil–structure interaction; Seismic isolation; Soil stratum

1. Introduction

In recent years, the seismic analysis of bridge structures has received considerable attention. As a result, a lot of improvements have been made mainly since the 1971 San Fernando earthquake [1,2]. A great number of research programs concerning the dynamic response of bridges under seismic excitation have resulted in the development of both simple analytical approaches and elaborate design procedures [3,4]. Furthermore, representative seismic analysis and design methods can be found in many review articles and textbooks [5–8].

Although soil–structure interaction results in a significant modification of the system properties, which in turn alter its seismic response, most current analysis methods that are either used or recommended in design codes (e.g. Caltrans, Seismic Design References, 1994) do not account for it. This discrepancy can be primarily attributed to numerous difficulties including the complexity of the problem, scarce pertinent experimental data and the lack of an easy-to-use design procedure. On the other hand, the necessity of incorporating soil–structure interaction in the design of a wide class of bridge structures has been pointed out by several post-earthquake investigations, experimental and analytical studies (e.g. The Northridge Earthquake, Post-Earthquake Investigation Report, Caltrans, 1994).

On the contrary, the work that has been carried out on the subject of seismic isolation is surely greater [6,9]. Usually, the design of regular bridges using the seismic isolation method involves the performance of an equivalent linear quasistatic or dynamic analysis, that assumes the determination of an equivalent viscous damping ratio or 'composite damping ratio' of the bridge. The composite damping ratio is based on the component damping ratios including the equivalent viscous damping ratios of the isolation bearings and the

* Corresponding authors. Tel.: +30-1-699-0041/42/44; fax: +30-1-699-0044.

E-mail addresses: tvlassis@ath.forthnet.gr (A.G. Vlassis), spyrakos@hol.gr (C.C. Spyrakos).

0045-7949/01/$ - see front matter
PII: S0045-7949(01)00105-5

viscous damping ratios of the piers, if the piers are designed to remain elastic during a major earthquake [10–12]. However, there are a lot of uncertainties and inconsistencies in determining the composite damping ratio of a seismically isolated bridge. Turkington et al. assumed that the system damping ratio is equal to the sum of the equivalent damping ratio of the isolation bearings and the 5% viscous damping ratio of the piers, while according to AASHTO [1], the contribution of the stiffness and damping of the piers is neglected. Approaches based on the modal strain energy method [13–15] are adopted by the Japanese Public Works Research Institute [16] and Caltrans [17].

The objective of this study is twofold: first, to estimate the effect of soil–structure interaction on the dynamic performance of a seismically isolated bridge pier placed on a shallow soil stratum overlying a rigid bedrock and, second, to develop a method that accounts for soil–structure interaction and can be easily applied to the preliminary design of this type of bridges. Since piers together with the abutments are the most critical bridge components in assuring the integrity of bridges during earthquakes, the study is focused on the pier behavior only. The relative significance that several bridge–soil system parameters have in designs with consideration of soil–structure interaction is examined and suggestions that can lead to more economical and safer isolated pier design are presented.

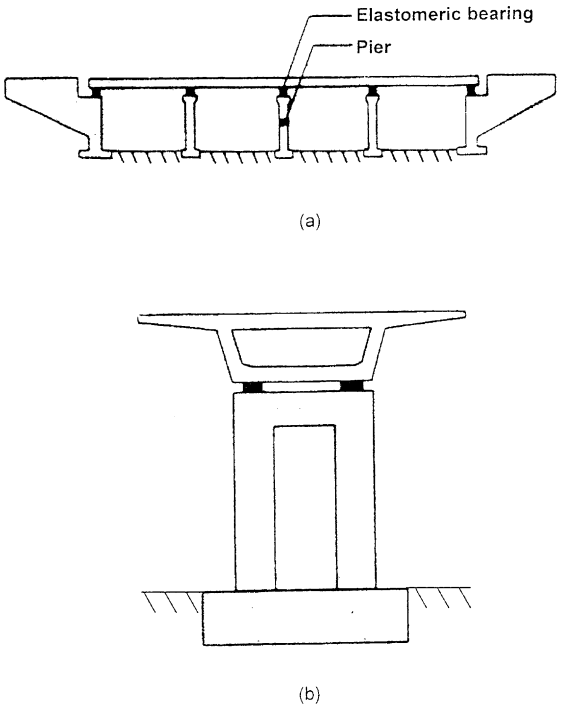

Fig. 1. Seismically isolated regular bridge elevation: (a) longitudinal and (b) transverse.

2. Bridge–soil system

The bridge–soil system representing a bridge that is excited in the longitudinal direction is depicted in Fig. 1. The piers are founded on a soil stratum that has practically identical properties along its depth and is overlying a rigid bedrock. The foundations are assumed to be massless and surface, while the mass of the piers is significantly smaller than the mass of the tributary bridge deck. Complying also with the concept of vibration isolation design, all the bridge components, other than the isolation bearings that are characterized by elastoplastic behavior, are assumed to remain elastic during an earthquake event in this paper. The height and the lumped mass at the top of its pier are denoted as h and m_s, respectively. The pier is characterized by an elastic stiffness k_s and viscous damping coefficient c_s. The isolation bearing is characterized by an effective stiffness k_b and equivalent viscous damping coefficient c_b. The tributary mass m_b of the corresponding bridge deck for each pier is assumed to be lumped above the bearing. In order to simplify the analysis, all piers are identical in size and stiffness. Further simplification considers a rigid deck and elimination of the rotational degrees of freedom at the top of the piers with very little sacrifice in computational accuracy [3]. Furthermore, as shown in Fig. 1, the bridge structure under consideration consists of relatively short spans and, therefore, the effects of non-uniform input motions due to different soil conditions across the bridge foundation are not taken into account.

The soil supporting the piers is modeled as a system of two springs and corresponding dashpots acting in the horizontal and rotational directions. The material damping in the soil is hysteretic and is characterized by a damping ratio ζ_g. The radiation (geometric) damping, which is developed through wave propagation emanating from the foundation in all directions of the soil strata, is viscous with damping ratios ζ_h and ζ_r, for the horizontal and rocking motions, respectively.

Under these assumptions, the dynamic response of a seismically isolated bridge pier with the corresponding part of the bridge deck at its top can be modeled with the aid of the shown in Fig. 2. It should be noted that the development of the four-degree-of-freedom system is based on the bridge–soil system presented in Ref. [18]. The four degrees of freedom include the horizontal displacement amplitude u_o of the foundation relative to the free-field motion, the rotational amplitude φ of the system at the foundation level, the amplitude of the relative displacement u_s of the pier lumped mass, and the amplitude of the relative displacement u_b of the lumped mass of the bridge super-structure.

3. Method of analysis

3.1. Equations of motion

Assuming the ground motion to be harmonic $u_g e^{i\omega t}$, the amplitudes of the horizontal force P_h and moment M_r that develop at the base of the pier can be written in the following form [4,18]:

$$P_h = k_h(1 + 2\zeta_h i + 2\zeta_g i)u_o \tag{1}$$

$$M_r = k_r(1 + 2\zeta_r i + 2\zeta_g i)\varphi \tag{2}$$

where:

$$\zeta_h = \frac{\omega c_h}{2k_h} \qquad \zeta_r = \frac{\omega c_r}{2k_r} \tag{3}$$

Furthermore, the circular frequencies ω_h and ω_r of the soil, pertaining to a fixed base bridge–soil system, follow from:

$$\omega_h^2 = \frac{k_h}{m_b + m_s} \qquad \omega_r^2 = \frac{k_r}{(m_b + m_s)h^2} \tag{4}$$

Similarly, the corresponding dynamic characteristics for the fixed base pier are given by:

$$\zeta_s = \frac{\omega c_s}{2k_s} \qquad \zeta_b = \frac{\omega c_b}{2k_b} \tag{5}$$

$$\omega_s^2 = \frac{k_s}{m_b + m_s} \qquad \omega_b^2 = \frac{k_b}{m_b} \tag{6}$$

Equilibrium of the horizontal forces acting on m_b and m_s, as well as equilibrium of the horizontal forces and moments at the base of the pier lead to the equations of motion of the pier–soil system:

$$\begin{bmatrix} \frac{\omega_b^2}{\omega^2}(1+2\zeta_b i)-1 & -\frac{\omega_b^2}{\omega^2}(1+2\zeta_b i) & -1 & -1 \\ -\frac{\omega_b^2}{\omega^2}(1-\gamma)(1+2\zeta_b i) & \frac{\omega_s^2}{\omega^2}(1+2\zeta_s i)+\frac{\omega_b^2}{\omega^2}(1-\gamma)(1+2\zeta_b i)-\gamma & -\gamma & -\gamma \\ \gamma-1 & -\gamma & \frac{\omega_h^2}{\omega^2}(1+2\zeta_h i+2\zeta_g i)-1 & -1 \\ \gamma-1 & -\gamma & -1 & \frac{\omega_r^2}{\omega^2}(1+2\zeta_r i+2\zeta_g i)-1 \end{bmatrix} \times \begin{Bmatrix} u_b \\ u_s \\ u_o \\ h\varphi \end{Bmatrix} = \begin{Bmatrix} 1 \\ \gamma \\ 1 \\ 1 \end{Bmatrix} u_g \tag{7}$$

where the mass ratio γ is defined as:

$$\gamma = \frac{m_s}{m_b + m_s} \tag{8}$$

Only u_b and u_s of the four degrees of freedom in Eq. (7) are dynamic, since the pier is assumed to be founded on the soil stratum through a massless foundation and therefore no inertia force develops at its base. As a consequence, an equivalent two-degree-of-freedom system can be derived from the four-degree-of-freedom model such that, when excited by base excitation $\tilde{u}_g$, its dynamic response coincides to that of the initial system. The equations of motion of the equivalent two-degree-of-freedom system can be written as:

$$\left([\widetilde{K}] + i[\tilde{\zeta}]\right)\begin{Bmatrix} u_b \\ u_s \end{Bmatrix} = \begin{Bmatrix} \frac{\omega^2}{\omega_b^2} \\ \gamma\frac{\omega^2}{\omega_s^2} \end{Bmatrix}\tilde{u}_g \tag{9}$$

where:

$$([\widetilde{K}] + i[\tilde{\zeta}]) = \begin{bmatrix} 1 + 2\tilde{\zeta}_b i - \frac{\omega^2}{\omega_b^2} & -(1 + 2\tilde{\zeta}_b i) \\ -\frac{\omega_b^2}{\omega_s^2}(1-\gamma)(1+2\tilde{\zeta}_b i) & 1 + 2\tilde{\zeta}_s i + \frac{\omega_b^2}{\omega_s^2}(1-\gamma)(1+2\tilde{\zeta}_b i) - \gamma\frac{\omega^2}{\omega_s^2} \end{bmatrix} \tag{10}$$

It should be noted that, if the pier mass m_s was neglected, Eq. (9) would reduce to the equation of motion of a single-degree-of-freedom system. In this case, the relevant parameters of the equivalent structure would be its tributary deck mass, its effective global stiffness and its effective global damping [6]. This procedure is generally applicable to very simple bridges and to a preliminary design phase of bridges for which the coupling effects of the deck can be neglected.

3.2. Modal properties of equivalent system

Based on the system of Eq. (9), the undamped natural frequencies and natural modes of the equivalent

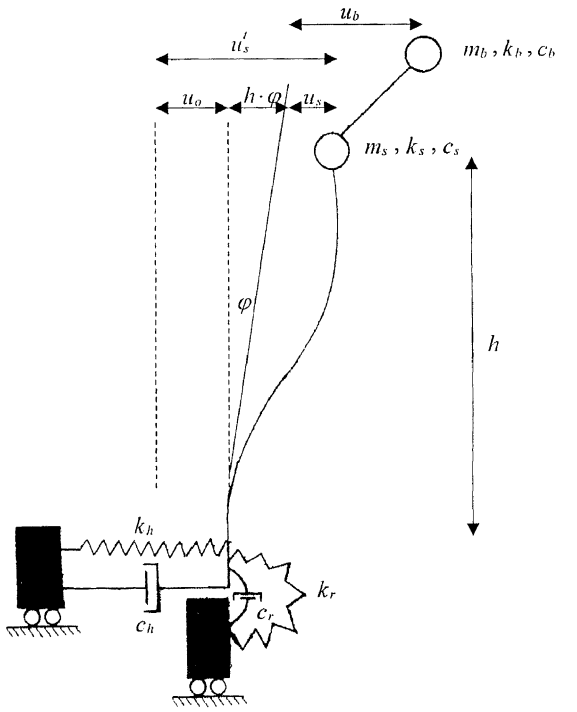

Fig. 2. Four-degree-of-freedom system to horizontal excitation.

two-degree-of-freedom system can be derived by setting $\tilde{\zeta}_b = \tilde{\zeta}_s = 0$:

$$\begin{bmatrix} 1-\frac{\widetilde{\omega}_m^2}{\widetilde{\omega}_b^2} & -1 \\ -\frac{\widetilde{\omega}_b^2}{\widetilde{\omega}_s^2}(1-\gamma) & 1+\frac{\widetilde{\omega}_b^2}{\widetilde{\omega}_s^2}(1-\gamma)-\gamma\frac{\widetilde{\omega}_m^2}{\widetilde{\omega}_s^2} \end{bmatrix}\{\widetilde{\Phi}^m\} = 0 \quad m = 1,2 \tag{11}$$

where $\widetilde{\omega}_m^2$, $m = 1,2$ are the natural frequencies corresponding to the isolation and structural modes, respectively, and:

$$\{\widetilde{\Phi}^m\} = \begin{Bmatrix} \widetilde{\Phi}_b^m \\ \widetilde{\Phi}_s^m \end{Bmatrix} \tag{12}$$

are the corresponding mode shape vectors.

The characteristic equation for determining the natural frequencies can be deduced from the system of Eq. (11):

$$\gamma\widetilde{\omega}_m^4 - \widetilde{\omega}_b^2\left(1+\frac{1-\gamma}{\widetilde{R}_s}\right)\widetilde{\omega}_m^2 + \frac{1-\gamma}{\widetilde{R}_s}\widetilde{\omega}_b^4 = 0 \tag{13}$$

where $\widetilde{R}_s$ denotes the stiffness ratio of the equivalent system that is equal to the effective stiffness of the isolation bearing $\tilde{k}_b$ divided by the elastic stiffness of the pier $\tilde{k}_s$:

$$\widetilde{R}_s = \frac{\tilde{k}_b}{\tilde{k}_s} \tag{14}$$

Therefore, the frequency ratio can be expressed as:

$$\frac{\widetilde{\omega}_b^2}{\widetilde{\omega}_s^2} = \frac{\widetilde{R}_s}{(1-\gamma)} \tag{15}$$

Solving Eq. (13) for the natural frequencies, we obtain:

$$\widetilde{\omega}_{1,2}^2 = \frac{\left(1+\frac{1-\gamma}{\widetilde{R}_s}\right) \pm \sqrt{\left(1+\frac{1-\gamma}{\widetilde{R}_s}\right)^2 - 4\gamma\frac{1-\gamma}{\widetilde{R}_s}}}{2\gamma}\widetilde{\omega}_b^2 \tag{16}$$

Setting $m = 1$ and $m = 2$ successively in Eq. (11), the mode shape vectors corresponding to the isolation and structural modes are determined, respectively, by:

$$\{\widetilde{\Phi}^1\} = \begin{Bmatrix} \widetilde{\Phi}_b^1 \\ \widetilde{\Phi}_s^1 \end{Bmatrix} = \begin{Bmatrix} 1 \\ 1-\widetilde{\omega}_1^2/\widetilde{\omega}_b^2 \end{Bmatrix} = \begin{Bmatrix} 1 \\ 1-\tilde{\alpha}_1 \end{Bmatrix} \quad \text{where:} \quad \tilde{\alpha}_1 = \frac{\widetilde{\omega}_1^2}{\widetilde{\omega}_b^2} \tag{17a}$$

$$\{\widetilde{\Phi}^2\} = \begin{Bmatrix} \widetilde{\Phi}_b^2 \\ \widetilde{\Phi}_s^2 \end{Bmatrix} = \begin{Bmatrix} 1 \\ 1-\widetilde{\omega}_2^2/\widetilde{\omega}_b^2 \end{Bmatrix} = \begin{Bmatrix} 1 \\ 1-\tilde{\alpha}_2 \end{Bmatrix} \quad \text{where:} \quad \tilde{\alpha}_2 = \frac{\widetilde{\omega}_2^2}{\widetilde{\omega}_b^2} \tag{17b}$$

Furthermore, the modal participation factors are given by:

$$\widetilde{\psi}_1 = \frac{\{\widetilde{\Phi}^1\}^T[\widetilde{M}]\{r\}}{\{\widetilde{\Phi}^1\}^T[\widetilde{M}]\{\widetilde{\Phi}^1\}} = \frac{\begin{Bmatrix} 1 & 1-\tilde{\alpha}_1 \end{Bmatrix}\begin{bmatrix} m_b & 0 \\ 0 & m_s \end{bmatrix}\begin{Bmatrix} 1 \\ 1 \end{Bmatrix}}{\begin{Bmatrix} 1 & 1-\tilde{\alpha}_1 \end{Bmatrix}\begin{bmatrix} m_b & 0 \\ 0 & m_s \end{bmatrix}\begin{Bmatrix} 1 \\ 1-\tilde{\alpha}_1 \end{Bmatrix}} = \frac{(1-\gamma)+(1-\tilde{\alpha}_1)\gamma}{(1-\gamma)+(1-\tilde{\alpha}_1)^2\gamma} \tag{18a}$$

$$\widetilde{\psi}_2 = \frac{\{\widetilde{\Phi}^2\}^T[\widetilde{M}]\{r\}}{\{\widetilde{\Phi}^2\}^T[\widetilde{M}]\{\widetilde{\Phi}^2\}} = \frac{\begin{Bmatrix} 1 & 1-\tilde{\alpha}_2 \end{Bmatrix}\begin{bmatrix} m_b & 0 \\ 0 & m_s \end{bmatrix}\begin{Bmatrix} 1 \\ 1 \end{Bmatrix}}{\begin{Bmatrix} 1 & 1-\tilde{\alpha}_2 \end{Bmatrix}\begin{bmatrix} m_b & 0 \\ 0 & m_s \end{bmatrix}\begin{Bmatrix} 1 \\ 1-\tilde{\alpha}_2 \end{Bmatrix}} = \frac{(1-\gamma)+(1-\tilde{\alpha}_2)\gamma}{(1-\gamma)+(1-\tilde{\alpha}_2)^2\gamma} \tag{18b}$$

The variation of the participation factors with the stiffness ratio $\widetilde{R}_s$ is plotted in Fig. 3. It can be easily observed that $\widetilde{\psi}_1 \cong 1.00$ and $\widetilde{\psi}_2 \cong 0.00$ for the whole range of the stiffness ratio, i.e. the contribution of the

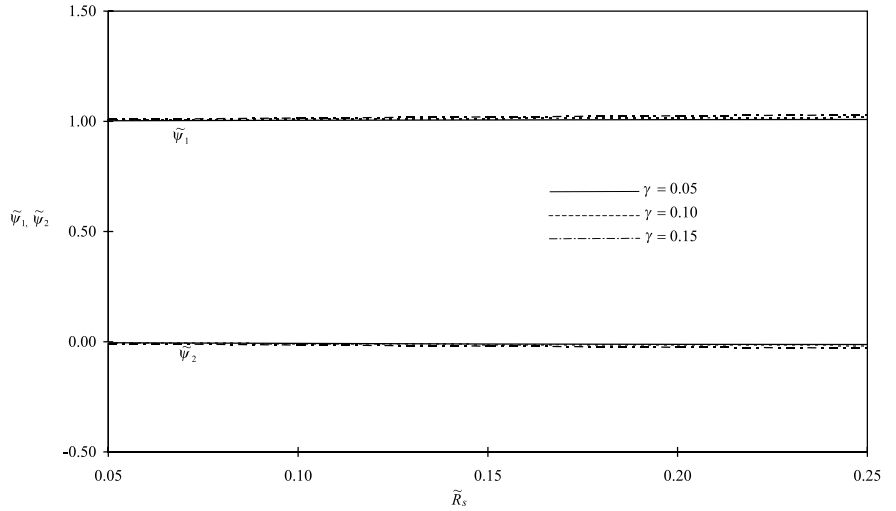

Fig. 3. Participation factors of isolation and structural modes.

structural mode $\{\widetilde{\Phi}^2\}$ can be neglected compared to that of the isolation mode $\{\widetilde{\Phi}^1\}$. Therefore, the isolation mode dominates the response of the system if the two natural modes are well separated. As a consequence, the first modal damping ratio $\tilde{\zeta}_1$, that is equal to the "composite damping ratio" of the system, is sufficient to express the behavior of the pier with adequate accuracy, as far as damping is concerned. In other words, the first modal damping ratio $\tilde{\zeta}_1$ is more important than the second modal damping ratio $\tilde{\zeta}_2$ when determining the seismic response of a seismically isolated bridge using the linear analysis method.

3.3. Circular frequencies and damping ratios of equivalent system

In correspondence to the equivalent system, the stiffness and the frequency ratios of the initial four-degree-of-freedom system can be expressed as follows:

$$R_s = \frac{k_b}{k_s} \quad \frac{\omega_b^2}{\omega_s^2} = \frac{R_s}{(1-\gamma)} \tag{19}$$

It should be noted that the concept of the equivalent two-degree-of-freedom system is based on the assumption of maintaining the same mass m_s for the pier and m_b for the isolation bearing as in the four-degree-of-freedom system. Furthermore, in order to assure that the two undamped systems have the same dynamic response, the relative displacement amplitudes u_b and u_s should be equal at resonance in both the initial and the equivalent systems. Therefore, performing a series of algebraic calculations, the circular frequencies of the isolation bearing and the pier in the equivalent system are, respectively, given by [19]:

$$\widetilde{\omega}_b^2 = \frac{\omega_s^2}{\frac{1-\gamma}{R_s}\left[1+\frac{1}{1+\gamma}\left(\frac{k_s}{k_h}+\frac{k_s h^2}{k_r}\right)\right]} \tag{20a}$$

$$\widetilde{\omega}_s^2 = \frac{\omega_s^2}{1+\frac{1}{\gamma+1}\left(\frac{k_s}{k_h}+\frac{k_s h^2}{k_r}\right)} \tag{20b}$$

According to the practical design examples that can be found in the Japanese Isolation Design Manual [20], three mass ratios equal to 0.05, 0.10 and 0.15 are assumed and the stiffness ratios are assumed to be within the range between 0.02 and 0.25. It can be easily concluded from Eqs. (20a) and (20b) that the circular frequencies $\widetilde{\omega}_b$ and $\widetilde{\omega}_s$ of the isolation bearing and the pier, respectively, in the equivalent system including soil–structure interaction are always smaller than the circular frequency ω_s of the pier in the initial fixed base structure.

Including damping and following the same procedure, the damping ratios matrix $\lfloor\tilde{\zeta}\rfloor$ of the equivalent system can be derived [19]:

$$[\tilde{\zeta}] = \begin{bmatrix} \tilde{\zeta}_{b_{11}} & -\tilde{\zeta}_{b_{12}} \\ -\tilde{\zeta}_{b_{21}} & \tilde{\zeta}_{b_{22}}+\frac{1}{\widetilde{R}_s}\tilde{\zeta}_{s_{22}} \end{bmatrix} \tag{21}$$

The analytical expressions for the four terms of the damping ratios matrix $\lfloor\tilde{\zeta}\rfloor$ are given in Appendix A.

4. Assessment of soil–structure interaction

Regarding the dynamic behavior of the soil, it is well established that, contrary to the stiffness and the damping of bridge super- and sub-structures, soil stiffness and damping characteristics largely depend on the frequency content of the externally applied loads.

However, for design purposes, the following frequency independent expressions can be used in order to evaluate the soil stiffness and damping coefficients of a rigid, circular, massless foundation on soil strata [21,22]:

$$k_{\mathrm{h}} = \frac{8G\alpha}{2-\nu}\left(1+\frac{1}{2\widetilde{H}}\right) \qquad c_{\mathrm{h}} = \frac{4.6\alpha^2}{2-\nu}\rho V_{\mathrm{s}} \tag{22a}$$

$$k_{\mathrm{r}} = \frac{8G\alpha^3}{3(1-\nu)}\left(1+\frac{1}{6\widetilde{H}}\right) \qquad c_{\mathrm{r}} = \frac{0.4\alpha^4}{1-\nu}\rho V_{\mathrm{s}} \tag{22b}$$

where α is the radius of the circular foundation, H is the depth of the soil stratum overlying a rigid bedrock and $\widetilde{H} = H/\alpha$. The expressions (22a) and (22b) are also valid for the limiting case of a very deep soil stratum, in which case $\widetilde{H}$ becomes infinite and the terms involving $\widetilde{H}$ are zero. In order to evaluate the effect of soil–structure interaction on the bridge model portrayed in Fig. 2, the system dynamic properties are expressed in terms of the following dimensionless parameters:

$$\bar{s} = \frac{\omega_{\mathrm{s}} h}{V_{\mathrm{s}}}, \quad \bar{h} = \frac{h}{\alpha} \text{ and } \bar{m} = \frac{m_{\mathrm{b}} + m_{\mathrm{s}}}{\rho\alpha^3} \tag{23}$$

With the aid of these dimensionless parameters, Eqs. (20a) and (20b) are transformed to [19]:

$$\frac{\widetilde{\omega}_{\mathrm{b}}^2}{\omega_{\mathrm{s}}^2} = \frac{1}{\frac{1-\gamma}{\widetilde{R}_{\mathrm{s}}}\eta} \tag{24a}$$

$$\frac{\widetilde{\omega}_{\mathrm{s}}^2}{\omega_{\mathrm{s}}^2} = \frac{1}{\eta} \tag{24b}$$

where:

$$\eta = 1 + \frac{1}{\gamma+1}\frac{\bar{s}^2\bar{m}}{8}\left[\frac{2-\nu}{\bar{h}^2\left(1+\frac{1}{2\bar{H}}\right)} + \frac{3(1-\nu)}{1+\frac{1}{6\bar{H}}}\right]$$

Furthermore, combining Eqs. (16) and (24a) we obtain:

$$\frac{\widetilde{\omega}_1^2}{\omega_{\mathrm{s}}^2} = \frac{R_{\mathrm{s}}}{\widetilde{R}_{\mathrm{s}}}\frac{1}{\eta}\lambda \tag{25}$$

where:

$$\lambda = \frac{\left(\frac{\widetilde{R}_{\mathrm{s}}}{1-\gamma}+1\right) - \sqrt{\left(\frac{\widetilde{R}_{\mathrm{s}}}{1-\gamma}+1\right)^2 - 4\gamma\frac{\widetilde{R}_{\mathrm{s}}}{1-\gamma}}}{2\gamma}$$

It should be noted that if the fundamental period $\widetilde{T}_1$ of the equivalent bridge–soil system is greater than the natural period $T_{\mathrm{ss}} = 4H/V_{\mathrm{s}}$ of the soil stratum (i.e. $\widetilde{T}_1 > 4H/V_{\mathrm{s}}$), the contribution of radiation damping in the soil is practically insignificant. Therefore, based on Eqs. (23) and (25), radiation damping in the soil should be taken into account only when the following condition is satisfied:

$$\frac{2}{\pi}\frac{\overline{H}}{\bar{h}}\bar{s}\sqrt{\lambda\frac{1}{\eta}\frac{R_{\mathrm{s}}}{\widetilde{R}_{\mathrm{s}}}} \geqslant 1 \tag{26}$$

In consistency with Eq. (26), the damping ratios matrix of the equivalent system is evaluated at resonance and then used for the whole frequency range. Setting $\omega = \widetilde{\omega}_1$ and using the dimensionless parameters, the four terms of the damping ratios matrix $\lfloor\tilde{\zeta}\rfloor$ are rewritten in the form shown in Appendix B. The generalized damping ratios matrix is obtained by:

$$\lfloor\tilde{\zeta}^*\rfloor = \{\widetilde{\Phi}^i\}^{\mathrm{T}}\lfloor\tilde{\zeta}\rfloor\{\widetilde{\Phi}^j\} \quad i=1,2, \ \ j=1,2 \tag{27}$$

According to the approximate procedure proposed by Veletsos and Ventura [23], the transformation that diagonalizes the stiffness matrix is also able to diagonalize the damping ratios matrix. Consequently, neglecting the off-diagonal terms of this matrix leads to [19]:

From this generalized damping ratios matrix, the first modal damping ratio or composite damping ratio is derived in the following form [19]:

$$\lfloor\tilde{\zeta}^*\rfloor = \begin{bmatrix} \tilde{\zeta}_{\mathrm{b}_{11}} - (1-\tilde{\alpha}_1)(\tilde{\zeta}_{\mathrm{b}_{12}} + \tilde{\zeta}_{\mathrm{b}_{21}}) + (1-\tilde{\alpha}_1)^2\left(\tilde{\zeta}_{\mathrm{b}_{22}} + \frac{1}{\widetilde{R}_{\mathrm{s}}}\tilde{\zeta}_{\mathrm{s}_{22}}\right) & 0 \\ 0 & \tilde{\zeta}_{\mathrm{b}_{11}} - (1-\tilde{\alpha}_2)(\tilde{\zeta}_{\mathrm{b}_{12}} + \tilde{\zeta}_{\mathrm{b}_{21}}) + (1-\tilde{\alpha}_2)^2\left(\tilde{\zeta}_{\mathrm{b}_{22}} + \frac{1}{\widetilde{R}_{\mathrm{s}}}\tilde{\zeta}_{\mathrm{s}_{22}}\right) \end{bmatrix} \tag{28}$$

$$\tilde{\zeta}_1 = \tilde{\zeta}_{11}^* \Rightarrow \tilde{\zeta}_1 = \tilde{\zeta}_{\mathrm{b}_{11}} - (1-\tilde{\alpha}_1)(\tilde{\zeta}_{\mathrm{b}_{12}} + \tilde{\zeta}_{\mathrm{b}_{21}}) + (1-\tilde{\alpha}_1)^2\left(\tilde{\zeta}_{\mathrm{b}_{22}} + \frac{1}{\widetilde{R}_{\mathrm{s}}}\tilde{\zeta}_{\mathrm{s}_{22}}\right) \tag{29}$$

It should be also noted that, according to the correspondence principle, e.g., the ratio $R_{\mathrm{s}}/\widetilde{R}_{\mathrm{s}}$ is almost independent of the variation of soil stiffness and remains equal to unit for the whole range of $\bar{s}$.

4.1. Equivalent fundamental frequency and composite damping ratio

In order to assess the effect of soil–structure interaction on the dynamic response of seismically isolated bridge piers founded on a soil stratum overlying a rigid bedrock a series of parametric studies have been performed. For the evaluations shown in Fig. 4a and all the subsequent figures, the viscous damping ratio ζ_s of the pier is assumed to be 2.5%. The selected value of ζ_s characterizes reinforced concrete piers and is quite conservative as, according to Japanese Public Works Research Institute [16], the proposed damping ratios for the piers are presumed to be within the range 3–10%.

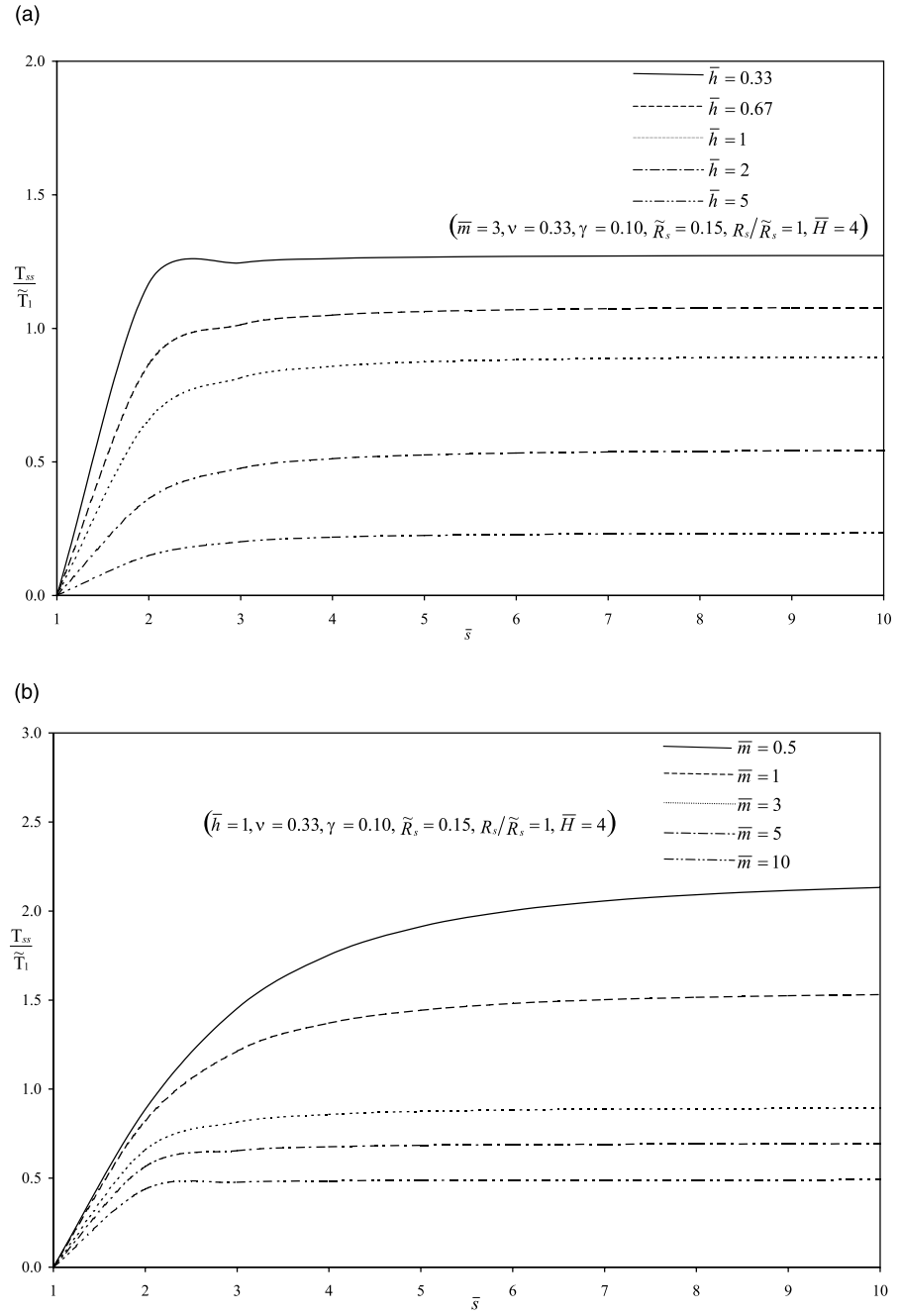

Fig. 4. Variation of $T_{ss}/\tilde{T}_1$ for representative $\bar{h}$ (a) and $\bar{m}$ (b).

Furthermore, the composite damping ratio $\tilde{\zeta}_1$ is evaluated for two characteristic values of the equivalent viscous damping ratio ζ_b of the bearing i.e. $\zeta_b = 5\%$ and $\zeta_b = 25\%$. The latter case refers to a lead rubber bearing, while $\zeta_b = 5\%$ corresponds to a natural rubber bearing. The Poisson's ratio v and the soil material damping ratio ζ_g are selected to be 0.33 and 5%, respectively, in order to realistically simulate moderately strong ground motions.

Fig. 4a and b depict the variation of $T_{ss}/\widetilde{T}_1$ as a function of $\bar{s}$ for representative values of $\bar{h}$ and $\bar{m}$, respectively, and for $\overline{H} = 4$, i.e. for a quite deep soil stratum compared to the radius of the circular foundation. As it can be easily observed in Fig. 4a, for the case of $\bar{m} = 3$, the ratio $T_{ss}/\widetilde{T}_1$ is greater than one and, therefore, radiation damping in the soil should be considered in design, only for very stiff piers ($\bar{h} = 0.33$, $\bar{h} = 0.67$). Similarly, referring to the curves of Fig. 4b, for a pier that its height is equal to its radius, i.e. $\bar{h} = 1$, $T_{ss}/\widetilde{T}_1$ exceeds unit only for very small values of $\bar{m}$ ($\bar{m} = 0.5$, $\bar{m} = 1$). In both figures, radiation damping should be taken into account for $\bar{s} > 1$, which corresponds to the fact that for most practical cases $\bar{s}$ varies between 3 and 8. In Fig. 5 the variation of the ratio $T_{ss}/\widetilde{T}_1$ is plotted versus $\bar{s}$ for the two extreme cases of $\bar{h} = 0.33$ and $\bar{m} = 0.5$. It can be easily deduced that even for very stiff piers that are characterized by a small value of $\bar{m}$, the depth of the soil stratum should be at least double the radius of the foundation in order to consider the beneficial effect of soil–structure interaction on the design of the pier. This can be mainly attributed to the fact that, for small values of $\overline{H}$, i.e. $\overline{H} < 2$, the rigid bedrock results in a significant decrease of the radiation damping by restricting the wave propagation far from the foundation. Furthermore, the phenomenon of soil amplification is rather possible to occur causing severe damage to the super-structure.

Fig. 6a and b show the variation of $\widetilde{\omega}_1/\omega_s$ as a function of $\bar{s}$ for $\overline{H} = 2$, 4 and several representative values of $\bar{h}$, $\bar{m}$, which are in consistency with the conclusions drawn from Figs. 4a, b and 5. The main trend observed is that decreasing the soil stiffness results in decreasing $\widetilde{\omega}_1/\omega_s$. It can be also seen that the effect of $\overline{H}$ is very small compared to the effect of the slenderness ratio $\bar{h}$. The decrease of slenderness ratio leads to smaller values of $\widetilde{\omega}_1/\omega_s$ and therefore soil–structure interaction effects are more pronounced in stiffer piers. On the contrary, unlike the case of a supporting semi-infinite soil medium [19], decreasing $\bar{m}$ also leads to a sharper decrease of $\widetilde{\omega}_1/\omega_s$. Since the variation of $\widetilde{\omega}_1/\omega_s$ is a criterion of the influence that soil–structure interaction has on the dynamic response of the seismically isolated pier, it can be deduced that soil–structure interaction should be considered in the design of stiff piers with a small value of $\bar{m}$ supported on flexible soil ($\bar{s} > 6$). Therefore, a higher predominant period of the system, $\widetilde{T}_1$, can be achieved by decreasing either the structural height or the system mass and by increasing the soil density.

In Fig. 7a and b, the first modal damping ratio $\tilde{\zeta}_1$ is plotted as a function of $\bar{s}$ for $\overline{H} = 2$, 4, $\bar{h} = 0.33$, 0.67 and $\bar{m} = 0.5$, 1. It is observed that, if radiation damping

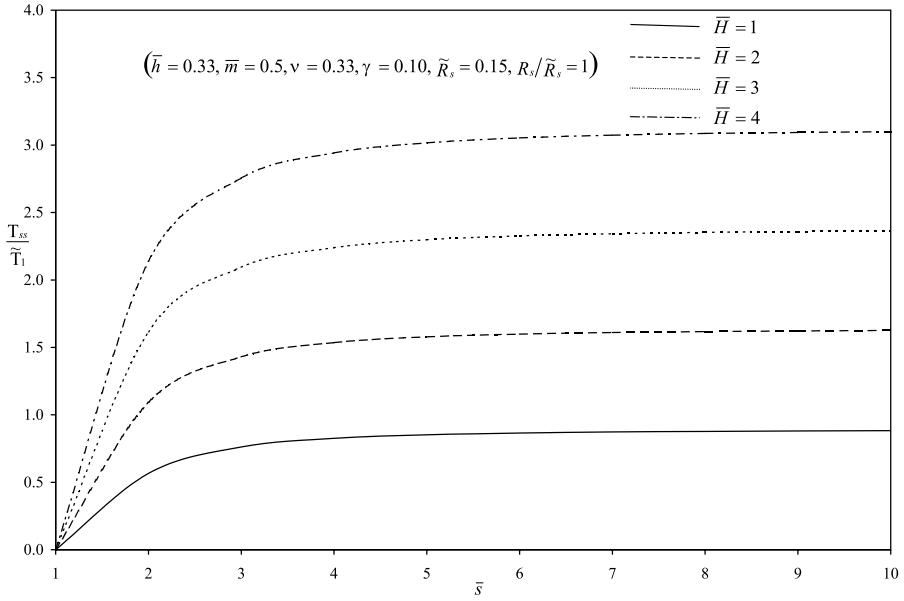

Fig. 5. Variation of $T_{ss}/\widetilde{T}_1$ for representative $\overline{H}$.

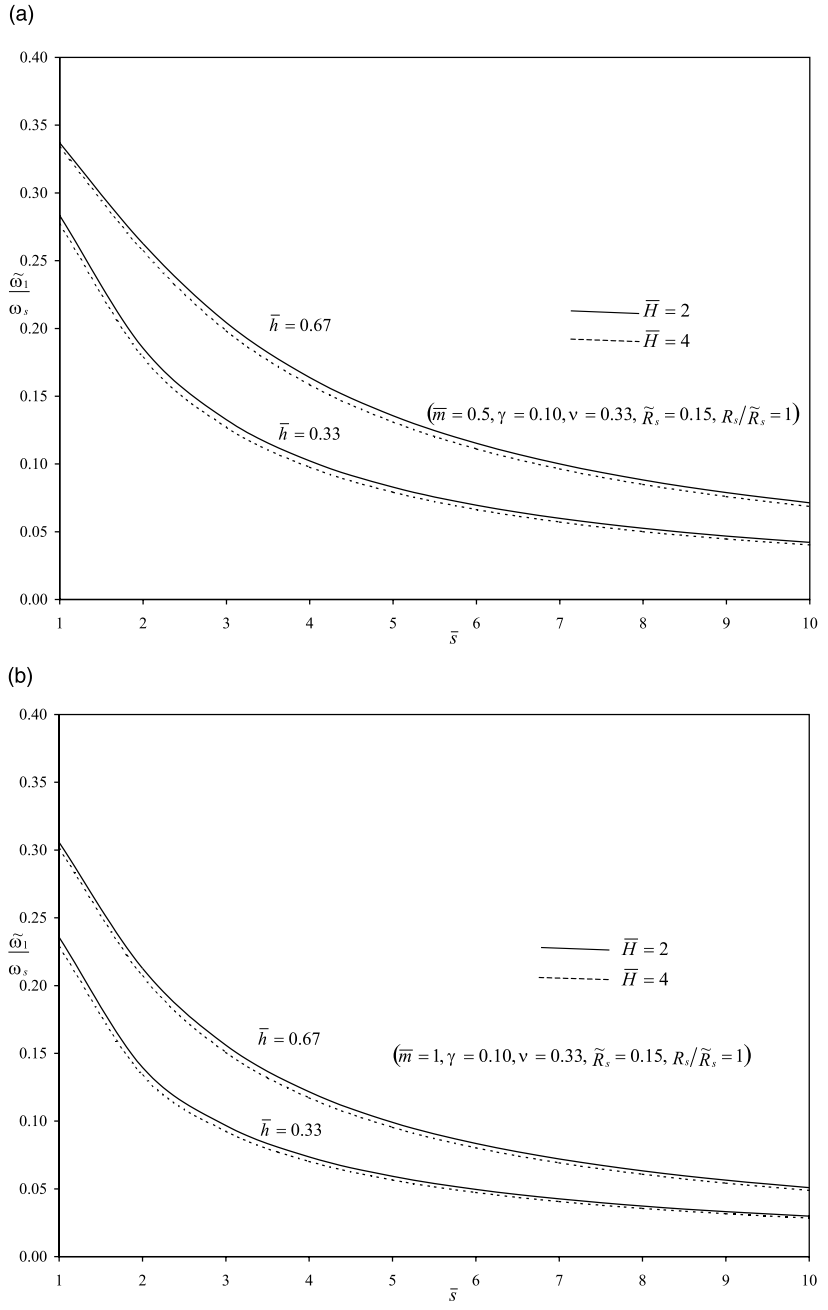

Fig. 6. Variation of frequency ratio $\tilde{\omega}_1/\omega_s$ for representative $\bar{h}$, $\overline{H}$ (a) $\bar{m} = 0.5$ and (b) $\bar{m} = 1$.

is considered, $\tilde{\zeta}_1$ increases for decreasing soil stiffness. The increase is more significant for squat piers, with predominantly translational mode shapes, that are characterized by a small value of $\bar{m}$. Further, the depth of the soil stratum has a negligible effect on the equivalent damping ratio. When radiation damping is not taken into account, there is no increase in the first modal damping ratio that remains constant for the whole range of $\bar{s}$. Similar trends can be also observed in Fig. 8a and b, which depict the variation of the composite damping ratio for $\zeta_b = 5\%$. In this case, the main difference is that the increase of $\tilde{\zeta}_1$ is a little higher approaching 15% for soft soil conditions. However, it should be noted that the increase of $\tilde{\zeta}_1$ is smaller than the relevant increase observed in the case of the soil medium [19] and it does not exceed 20% in any of the cases examined. This is

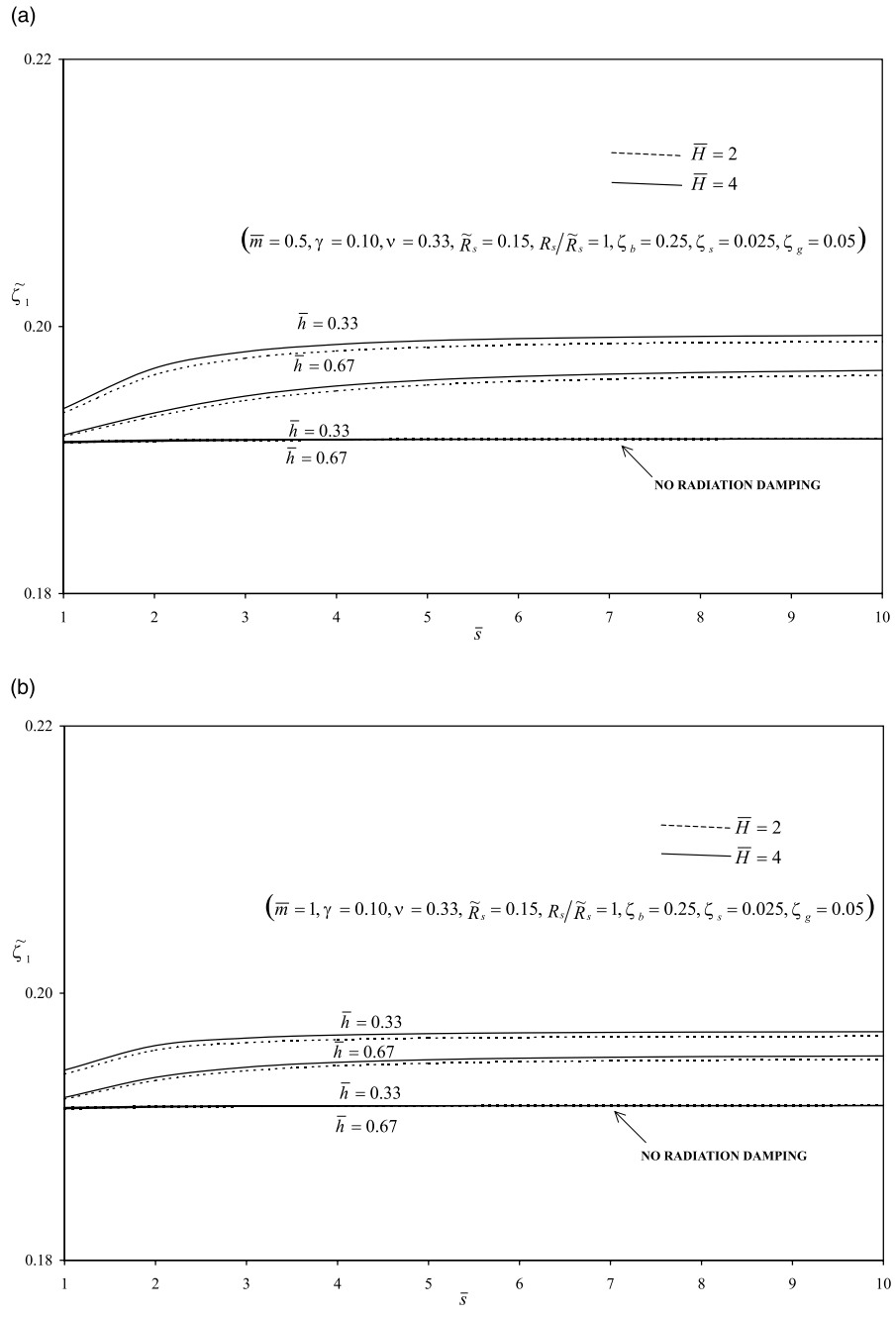

Fig. 7. Variation of composite damping ratio $\tilde{\zeta}_1$ for representative $\bar{h}$, $\bar{H}$ (a) $\bar{m} = 0.5$ and (b) $\bar{m} = 1$ ($\zeta_b = 25\%$).

attributed to the substantial reduction of damping, which is imposed by the rigid bedrock that restricts the emanation of waves away from the shallow stratum. Furthermore, it can be deducted that when soil–structure interaction is considered, the composite damping ratio is always smaller than the equivalent viscous damping ratio of isolation bearings and, therefore, the approaches of both AASHTO [1] and Turkington [10] for the evaluation of $\tilde{\zeta}_1$ are rather unconservative.

4.2. Seismic base shear

According to the AASHTO Guide Specification of Seismic Design of Highway Bridges [1], in the case that

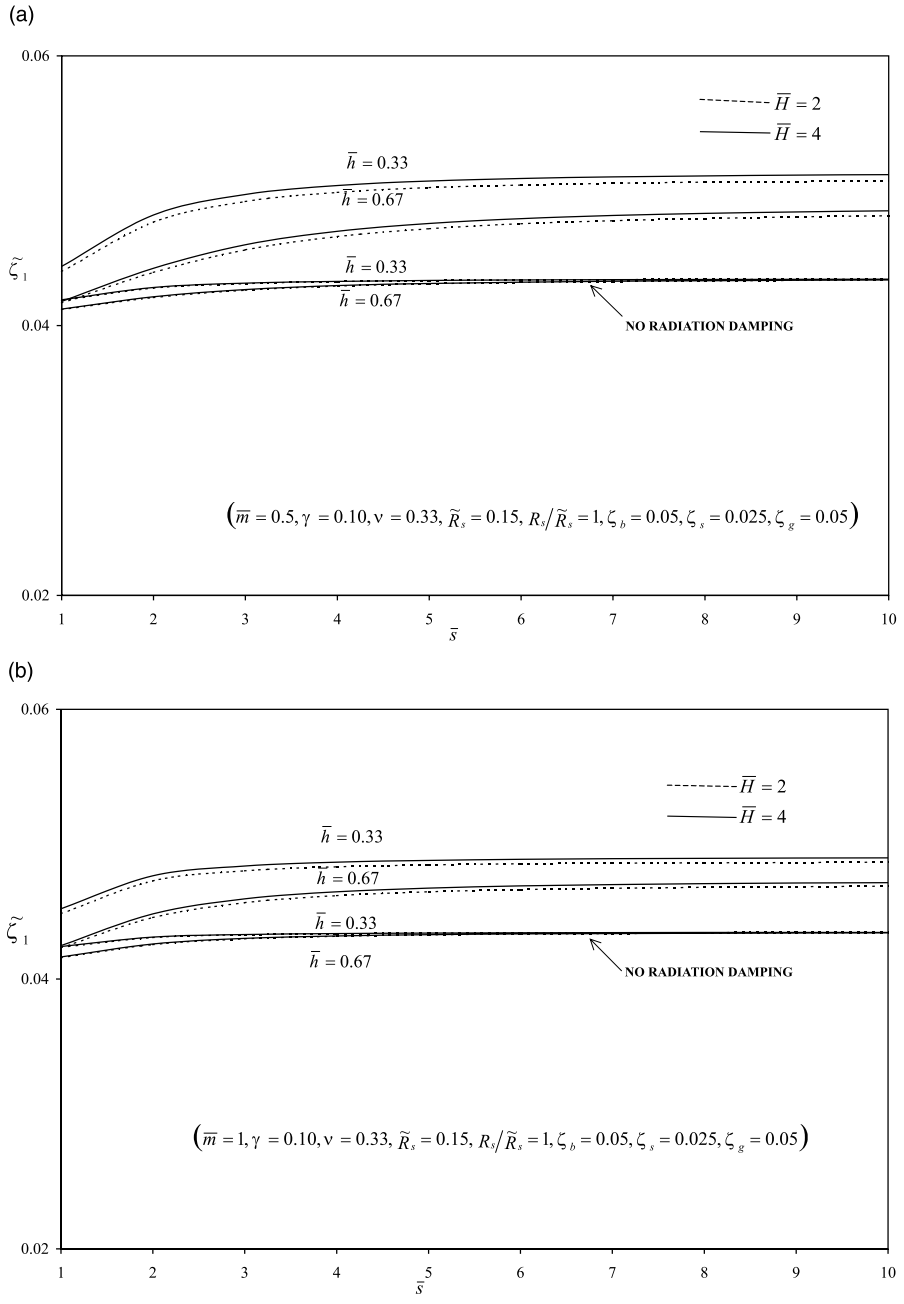

Fig. 8. Variation of composite damping ratio $\tilde{\zeta}_1$ for representative $\bar{h}$, $\bar{H}$ (a) $\bar{m} = 0.5$ and (b) $\bar{m} = 1$ ($\zeta_b = 5\%$).

soil–structure interaction is not considered in the design, the shear at the base of the pier can be evaluated from:

$$V = C_s W \tag{30}$$

where C_s and W denote the seismic design coefficient and the gravity weight associated with the pier, respectively. The seismic design coefficient can be obtained by the following expression:

$$C_s(T_1, \zeta_1) = 1.2 \frac{AS}{T_1^{2/3}} \tag{31}$$

As Eq. (31) indicates, $C_s(T_1, \zeta_1)$ depends on the fundamental period T_1 of the fixed base structure, the effective peak acceleration coefficient A and accounts for both the structural damping and the local soil conditions through the dimensionless coefficient S. However, it is

evident that S does not consider the effect of soil–structure interaction on the dynamic behavior of the pier. Introducing a seismic coefficient that takes soil–structure interaction into account, Eq. (30) should be rewritten as:

$$\widetilde{V} = C_s(\widetilde{T}_1, \tilde{\zeta}_1)W \tag{32}$$

where $\widetilde{T}_1$, $\tilde{\zeta}_1$ are the natural period and the first modal damping ratio of the equivalent two-degree-of-freedom system, respectively.

Assuming initially that the damping of the system is ζ_1 and the period is $\widetilde{T}_1$, Eq. (31) renders the following expression for $C_s(\widetilde{T}_1, \zeta_1)$:

$$C_s(\widetilde{T}_1, \zeta_1) = 1.2\frac{AS}{\widetilde{T}_1^{2/3}} \tag{33}$$

For the most currently encountered soil conditions subjected to moderate to strong ground motions, the values of C_s corresponding to different damping ratios $\tilde{\zeta}_1$, but to the same natural period $\widetilde{T}_1$, can be related to $C_s(\widetilde{T}_1, \zeta_1)$ through the approximate relationship [24]:

$$C_s(\widetilde{T}_1, \tilde{\zeta}_1) = C_s(\widetilde{T}_1, \zeta_1)\left(\frac{\zeta_1}{\tilde{\zeta}_1}\right)^{0.4} \tag{34}$$

Combining Eqs. (32)–(34), the ratio of the base shear $\widetilde{V}$ accounting for soil–structure interaction to the fixed base shear V, specified by the current AASHTO recommendations, can be expressed as:

$$\frac{\widetilde{V}}{V} = \left(\frac{T_1}{\widetilde{T}_1}\right)^{2/3}\left(\frac{\zeta_1}{\tilde{\zeta}_1}\right)^{0.4} \tag{35}$$

Expressing Eq. (35) in terms of the first natural frequency of the fixed base pier ω_1 and the equivalent two-degree-of-freedom system $\tilde{\omega}_1$, respectively, we obtain the following expression for the shear reduction factor:

$$\frac{\widetilde{V}}{V} = \left(\frac{\tilde{\omega}_1^2}{\omega_1^2}\right)^{1/3}\left(\frac{\zeta_1}{\tilde{\zeta}_1}\right)^{0.4} \tag{36}$$

In correspondence to the equivalent system, the first modal damping ratio of the fixed base seismically isolated pier is given by:

$$\zeta_1 = \zeta_b - (1-\alpha_1)(\zeta_b + \zeta_b) + (1-\alpha_1)^2\left(\zeta_b + \frac{1}{R_s}\zeta_s\right) \tag{37}$$

where α_1 is specified by:

$$\alpha_1 = \frac{\omega_1^2}{\omega_b^2} = \frac{\left(1+\frac{1-\gamma}{R_s}\right) - \sqrt{\left(1+\frac{1-\gamma}{R_s}\right)^2 - 4\gamma\frac{1-\gamma}{R_s}}}{2\gamma} \tag{38}$$

In order to assess the effect that accounting for soil–structure interaction may have on the current AASHTO design specifications, the shear reduction factor $\widetilde{V}/V$ can be also expressed in terms of the previously defined dimensionless parameters $\bar{s}$, $\bar{h}$, $\bar{m}$ and $\overline{H}$ [19]:

$$\frac{\widetilde{V}}{V} = \left(\frac{1}{\eta}\right)^{1/3}\left(\frac{\zeta_1}{\tilde{\zeta}_1}\right)^{0.4} \tag{39}$$

Fig. 9a and b depicts the variation of $\widetilde{V}/V$ as a function of $\bar{s}$ for $\overline{H} = 2, 4$ and for several representative values of $\bar{h}$, $\bar{m}$. The equivalent viscous damping ratio ζ_b of the isolation bearing, the viscous damping ratio ζ_s of the pier, and the soil material damping ratio ζ_g are assumed to be 25%, 2.5% and 5%, respectively. It should be noted that the case of $\zeta_b = 5\%$ was not examined since the predominant trends characterizing the variation of the composite damping ratio $\tilde{\zeta}_1$ for $\zeta_b = 25\%$ and $\zeta_b = 5\%$ were almost identical. As expected, it is observed that decreasing the soil stiffness results in smaller values of $\widetilde{V}/V$. However, a decrease in soil stiffness usually leads to an increase of the total displacement at the top of the pier relative to the base, which in turn may increase the secondary shear associated with P–δ effects. Such an increase is generally small and is usually neglected in analysis [5]. The decrease of the shear reduction factor is sharper in squat piers, at small values of $\bar{s}$ ($\bar{s} < 5$). This behavior is of major importance in the seismic design of bridges founded on stiff soil conditions. Furthermore, by comparing the solid and dotted curves, it can be deduced that the variation of $\overline{H}$ has an insignificant effect on $\widetilde{V}/V$ and thus it can be neglected in the design of seismically isolated bridge piers.

5. Conclusions

A theoretical study of soil–structure interaction in seismically isolated bridge piers placed on a shallow soil stratum overlying a rigid bedrock and subjected to horizontal seismic excitations has been conducted. In order to demonstrate the significant effect of soil–structure interaction on the longitudinal response of short span seismically isolated bridges, a simple structure–soil idealization, yet capable to capture the most salient features of the phenomenon, is adopted.

The main scope of this study was to identify when consideration of soil–structure interaction results in substantial differences from current design procedures. Therefore, a series of thorough parametric studies have been performed and led to: first, an assessment of the effect of soil–structure interaction on the seismic behavior of bridge piers and, second, an evaluation of the shear force that develops at the pier base including soil–structure interaction. It is worth noting that this study focused primarily on the evaluation of the effects of soil–structure interaction on the response of a single bridge pier. Further research is needed to examine the dynamic

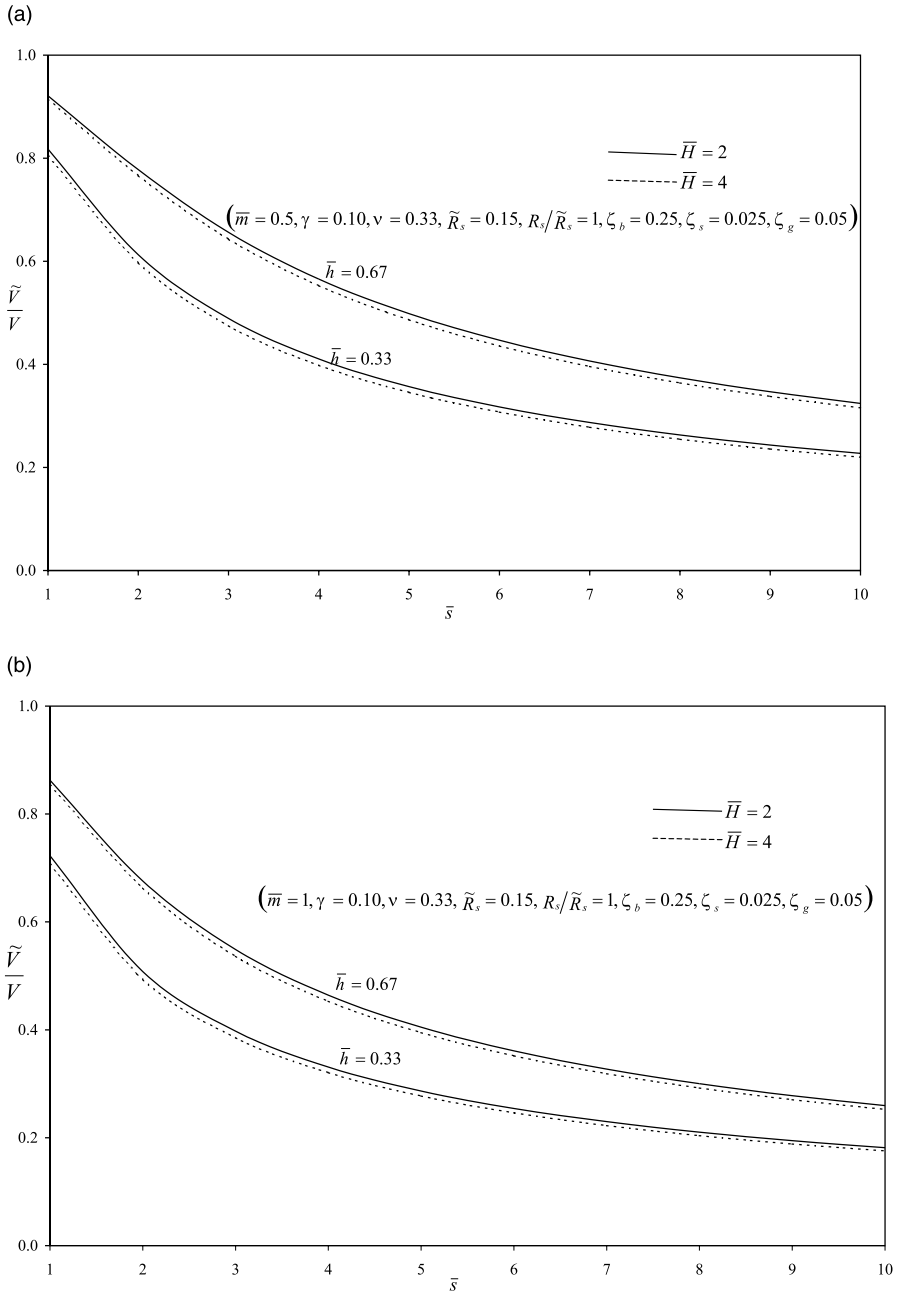

Fig. 9. Variation of shear reduction factor $\widetilde{V}/V$ for representative $\bar{h}$, $\overline{H}$ (a) $\bar{m} = 0.5$ and (b) $\bar{m} = 1$.

interaction between adjacent bridge piers in order to allow a more conclusive investigation of the necessity to incorporate soil–structure interaction in design of seismically isolated bridges.

The following conclusions emerge:

(1) The fundamental period of the bridge–soil system is significantly increased when soil–structure interaction is taken into account, especially when the isolation devices are not much more flexible than the supporting soil.

(2) Soil–structure interaction does not appear to play a major role as far as damping is concerned. This should be mainly attributed to the presence of the isolation bearings that cause a significant decrease in the total

stiffness of the system. As a consequence, the beneficial effect of soil–structure interaction on the seismic behavior of rather stiff structures is limited.

(3) Consideration of soil–structure interaction reduces the base shear force evaluated as recommended by the current AASHTO design procedures. The reduction is greater for bridge piers founded on stiff soil conditions.

Cases in which soil–structure interaction needs to be incorporated in seismically isolated bridge design are identified and ways to take advantage of soil–structure interaction in order to enhance the safety level and reduce design costs are suggested.

Appendix A

$$\begin{aligned}\tilde{\zeta}_{b_{11}} &= \left[1-\frac{\gamma}{\gamma+1}\left(\frac{\omega^2}{\omega_h^2}+\frac{\omega^2}{\omega_r^2}\right)\right]\zeta_b \\ &+\left[\frac{\gamma}{\gamma+1}\frac{\omega^2}{\omega_h^2}\left(1-\gamma\frac{\omega^2}{\omega_b^2}\right)\right]\zeta_h \\ &+\left[\frac{\gamma}{\gamma+1}\frac{\omega^2}{\omega_r^2}\left(1-\gamma\frac{\omega^2}{\omega_b^2}\right)\right]\zeta_r \\ &+\left[\frac{\gamma}{\gamma+1}\left(1-\gamma\frac{\omega^2}{\omega_b^2}\right)\left(\frac{\omega^2}{\omega_h^2}+\frac{\omega^2}{\omega_r^2}\right)\right]\zeta_g \end{aligned} \tag{A.1}$$

$$\begin{aligned}\tilde{\zeta}_{b_{12}} &= \left[1-\frac{\gamma}{\gamma+1}\left(\frac{\omega^2}{\omega_h^2}+\frac{\omega^2}{\omega_r^2}\right)\right]\zeta_b \\ &+\left[\frac{1}{\gamma+1}\frac{\omega_s^2}{\omega_b^2}\left(\frac{\omega^2}{\omega_h^2}+\frac{\omega^2}{\omega_r^2}\right)\right]\zeta_s \\ &+\left[\frac{1}{\gamma+1}\frac{\omega^2}{\omega_h^2}\left(\gamma-\frac{\omega_s^2}{\omega_b^2}-\gamma^2\frac{\omega^2}{\omega_b^2}\right)\right]\zeta_h \\ &+\left[\frac{1}{\gamma+1}\frac{\omega^2}{\omega_r^2}\left(\gamma-\frac{\omega_s^2}{\omega_b^2}-\gamma^2\frac{\omega^2}{\omega_b^2}\right)\right]\zeta_r \\ &+\left[\frac{1}{\gamma+1}\left(\gamma-\frac{\omega_s^2}{\omega_b^2}-\gamma^2\frac{\omega^2}{\omega_b^2}\right)\left(\frac{\omega^2}{\omega_h^2}+\frac{\omega^2}{\omega_r^2}\right)\right]\zeta_g \end{aligned} \tag{A.2}$$

$$\begin{aligned}\tilde{\zeta}_{b_{21}} &= \frac{1}{\widetilde{R}_s}\left\{\frac{\omega_b^2}{\omega_s^2}\left[(1-\gamma)+\frac{\gamma^2}{\gamma+1}\left(\frac{\omega^2}{\omega_h^2}+\frac{\omega^2}{\omega_r^2}\right)\right]\right\}\zeta_b \\ &+\frac{1}{\widetilde{R}_s}\left[\frac{\gamma^2}{\gamma+1}\frac{\omega^2}{\omega_h^2}\left(\gamma\frac{\omega^2}{\omega_s^2}-\frac{\omega_b^2}{\omega_s^2}\right)\right]\zeta_h \\ &+\frac{1}{\widetilde{R}_s}\left[\frac{\gamma^2}{\gamma+1}\frac{\omega^2}{\omega_r^2}\left(\gamma\frac{\omega^2}{\omega_s^2}-\frac{\omega_b^2}{\omega_s^2}\right)\right]\zeta_r \\ &+\frac{1}{\widetilde{R}_s}\left[\frac{\gamma^2}{\gamma+1}\left(\gamma\frac{\omega^2}{\omega_s^2}-\frac{\omega_b^2}{\omega_s^2}\right)\left(\frac{\omega^2}{\omega_h^2}+\frac{\omega^2}{\omega_r^2}\right)\right]\zeta_g \end{aligned} \tag{A.3}$$

$$\begin{aligned}\tilde{\zeta}_{b_{22}}+\frac{1}{\widetilde{R}_s}\tilde{\zeta}_{s_{22}} &= \frac{1}{\widetilde{R}_s}\left\{\frac{\omega_b^2}{\omega_s^2}\left[(1-\gamma)+\frac{\gamma^2}{\gamma+1}\left(\frac{\omega^2}{\omega_h^2}+\frac{\omega^2}{\omega_r^2}\right)\right]\right\}\zeta_b \\ &+\frac{1}{\widetilde{R}_s}\left[1-\frac{\gamma}{\gamma+1}\left(\frac{\omega^2}{\omega_h^2}+\frac{\omega^2}{\omega_r^2}\right)\right]\zeta_s \\ &+\frac{1}{\widetilde{R}_s}\left[\frac{\gamma}{\gamma+1}\frac{\omega^2}{\omega_h^2}\left(1-\gamma\frac{\omega_b^2}{\omega_s^2}+\gamma^2\frac{\omega^2}{\omega_s^2}\right)\right]\zeta_h \\ &+\frac{1}{\widetilde{R}_s}\left[\frac{\gamma}{\gamma+1}\frac{\omega^2}{\omega_r^2}\left(1-\gamma\frac{\omega_b^2}{\omega_s^2}+\gamma^2\frac{\omega^2}{\omega_s^2}\right)\right]\zeta_r \\ &+\frac{1}{\widetilde{R}_s}\left[\frac{\gamma}{\gamma+1}\left(1-\gamma\frac{\omega_b^2}{\omega_s^2}+\gamma^2\frac{\omega^2}{\omega_s^2}\right)\right. \\ &\left.\times\left(\frac{\omega^2}{\omega_h^2}+\frac{\omega^2}{\omega_r^2}\right)\right]\zeta_g \end{aligned} \tag{A.4}$$

Appendix B

$$\begin{aligned}\tilde{\zeta}_{b_{11}} &= \left[1-\gamma\lambda\left(1-\frac{R_s}{\widetilde{R}_s}\frac{1}{\eta}\right)\right]\zeta_b \\ &+\left\{\gamma\left[1-\frac{\gamma(1-\gamma)}{\widetilde{R}_s}\lambda\frac{1}{\eta}\right]\lambda\left(1-\frac{R_s}{\widetilde{R}_s}\frac{1}{\eta}\right)\right\}\zeta_g \\ &+\frac{\gamma}{\gamma+1}\left[1-\frac{\gamma(1-\gamma)}{\widetilde{R}_s}\lambda\frac{1}{\eta}\right]\left(\lambda\frac{R_s}{\widetilde{R}_s}\frac{1}{\eta}\sqrt{\lambda\frac{R_s}{\widetilde{R}_s}\frac{1}{\eta}}\kappa\right) \end{aligned} \tag{B.1}$$

$$\begin{aligned}\tilde{\zeta}_{b_{12}} &= \left[1-\gamma\lambda\left(1-\frac{R_s}{\widetilde{R}_s}\frac{1}{\eta}\right)\right]\zeta_b+\left[\frac{1-\gamma}{R_s}\lambda\left(1-\frac{R_s}{\widetilde{R}_s}\frac{1}{\eta}\right)\right]\zeta_s \\ &+\left[\left(\gamma-\frac{1-\gamma}{R_s}-\gamma^2\frac{1-\gamma}{R_s}\lambda\frac{1}{\eta}\right)\lambda\left(1-\frac{R_s}{\widetilde{R}_s}\frac{1}{\eta}\right)\right]\zeta_g \\ &+\frac{1}{\gamma+1}\left(\gamma-\frac{1-\gamma}{R_s}-\gamma^2\frac{1-\gamma}{R_s}\lambda\frac{1}{\eta}\right) \\ &\times\left(\lambda\frac{R_s}{\widetilde{R}_s}\frac{1}{\eta}\sqrt{\lambda\frac{R_s}{\widetilde{R}_s}\frac{1}{\eta}}\kappa\right) \end{aligned} \tag{B.2}$$

$$\begin{aligned}\tilde{\zeta}_{b_{21}} &= \frac{1}{\widetilde{R}_s}\left\{\frac{R_s}{1-\gamma}\left[(1-\gamma)+\gamma^2\lambda\left(1-\frac{R_s}{\widetilde{R}_s}\frac{1}{\eta}\right)\right]\right\}\zeta_b \\ &+\frac{1}{\widetilde{R}_s}\left[\gamma^2\left(\gamma\lambda\frac{R_s}{\widetilde{R}_s}\frac{1}{\eta}-\frac{R_s}{1-\gamma}\right)\lambda\left(1-\frac{R_s}{\widetilde{R}_s}\frac{1}{\eta}\right)\right]\zeta_g \\ &+\frac{1}{\widetilde{R}_s}\left[\frac{\gamma^2}{\gamma+1}\left(\gamma\lambda\frac{R_s}{\widetilde{R}_s}\frac{1}{\eta}-\frac{R_s}{1-\gamma}\right)\left(\lambda\frac{R_s}{\widetilde{R}_s}\frac{1}{\eta}\sqrt{\lambda\frac{R_s}{\widetilde{R}_s}\frac{1}{\eta}}\kappa\right)\right] \end{aligned} \tag{B.3}$$

$$\tilde{\zeta}_{b_{22}} + \frac{1}{\widetilde{R}_s}\tilde{\zeta}_{s_{22}} = \frac{1}{\widetilde{R}_s}\left\{\frac{R_s}{1-\gamma}\left[(1-\gamma)+\gamma^2\lambda\left(1-\frac{R_s}{\widetilde{R}_s}\frac{1}{\eta}\right)\right]\right\}\zeta_b + \frac{1}{\widetilde{R}_s}\left[1-\gamma\lambda\left(1-\frac{R_s}{\widetilde{R}_s}\frac{1}{\eta}\right)\right]\zeta_s + \frac{1}{\widetilde{R}_s}\left[\gamma\left(1-\frac{\gamma R_s}{1-\gamma}+\gamma^2\lambda\frac{R_s}{\widetilde{R}_s}\frac{1}{\eta}\right)\lambda\left(1-\frac{R_s}{\widetilde{R}_s}\frac{1}{\eta}\right)\right]\zeta_g + \frac{1}{\widetilde{R}_s}\left[\frac{\gamma}{\gamma+1}\left(1-\frac{\gamma R_s}{1-\gamma}+\gamma^2\lambda\frac{R_s}{\widetilde{R}_s}\frac{1}{\eta}\right) \times\left(\lambda\frac{R_s}{\widetilde{R}_s}\frac{1}{\eta}\sqrt{\lambda\frac{R_s}{\widetilde{R}_s}\frac{1}{\eta}}\kappa\right)\right] \quad \text{(B.4)}$$

where:

$$\kappa = \frac{\bar{s}^3\bar{m}}{\bar{h}}\left[0.036\frac{2-\nu}{\bar{h}^2\left(1+\frac{1}{2\bar{H}}\right)^2}+0.028\frac{1-\nu}{\left(1+\frac{1}{6\bar{H}}\right)^2}\right]$$

References

[1] Standard specifications for highway bridges, 15th ed. American Association of State Highway and Transportation Officials (AASHTO), USA, 1992.

[2] Eurocode 8. Earthquake resistant bridge structures, Part 2-Bridges, ENV 1998-2, 1994.

[3] Crouse CB, Hushmand B, Martin GR. Dynamic soil-structure interaction of a single span bridge. Earthquake Eng Struct Dyn 1987;15:711–29.

[4] Spyrakos CC. Assessment of SSI on the longitudinal seismic response of short span bridges. Eng Struct 1990;12:60–6.

[5] Okamoto S. Introduction to earthquake engineering. Tokyo: University of Tokyo Press; 1984.

[6] Priestley MNJ, Seible F, Calvi GM. Seismic design and retrofit of bridges. New York: John Wiley; 1996.

[7] Antes H, Spyrakos CC. Computer analysis and design of earthquake resistant structures, soil-structure interaction. Southampton: Computational Mechanics Publications; 1997, p. 271–332 [chapter 6].

[8] Elnashai AS. Conceptual seismic design of bridges. Proceedings of the Advanced Study Course on Seismic Risk, Edit. ITSAK, 1997. p. 545–63.

[9] Hwang JS, Chang KC, Tsai MH. Composite damping ratio of seismically isolated regular bridges. Eng Struct 1997;19(1):55–62.

[10] Turkington DH, Carr AJ, Cooke N, Moss PJ. Seismic design of bridges on lead-rubber bearings. J Struct Eng ASCE 1989;115(12):3000–16.

[11] Kelly JM. Earthquake-resistant design with rubber. London: Springer; 1993.

[12] Calvi GM, Pavese A. Conceptual design of isolation systems for bridge structures. Workshop on Problems in Highway Bridge Design. Thessaloniki, Greece, 1998.

[13] Ragget JD. Estimating damping of real structures. J Struct Div ASCE 1975;101:1823–35.

[14] Johnson CD, Keinholz DA. Finite element prediction of damping in structures with constrained viscoelastic layers. AIAA J 1982;20(9):1284–90.

[15] Soong TT, Lai ML. Correlation of experimental results with predictions of viscoelastic damping for a model structure. Proceedings of Damping 1991, Air Force Systems Command, Wright-Patterson Air Force Base, Ohio, FCB 1–7, 1991.

[16] Manual for Menshin design of highway bridges. Japanese Public Work Research Institute (JPWRI), Japan, 1992.

[17] Bridge design specifications. California Department of Transportation (CALTRANS), USA, 1983.

[18] Wolf JP. Dynamic soil–structure interaction. Englewood Cliffs, NJ: Prentice Hall; 1985.

[19] Vlassis AG. Effect of SSI on seismically isolated bridges. Bachelor thesis, NTUA, Athens, Greece, 1998.

[20] Japanese isolation design manual. Japanese Public Work Research Institute (JPWRI), Japan, 1992.

[21] Seismic design of highway bridge foundations, vol. I, Executive summary, vol. II, Design procedures and guidelines. Federal Highway Administration (FHWA), US Department of Transportation, USA, 1986.

[22] Gazetas G. Analysis of machine foundation vibrations: state of the art. Soil Dyn Earthquake Eng 1983;2:1–42.

[23] Veletsos AS, Ventura CE. Modal analysis of non-classically damped systems. Earthquake Eng Struct Dyn 1986; 14:217–43.

[24] Veletsos AS, Nair VV. Seismic interaction of structures on hysteretic foundations. J Struct Div ASCE 1975;101(ST1): 109–29.